

Exploring the Unexpected: Disharmonized Harmonic Pulsation Modes in High-Amplitude δ Scuti Stars

HUI-FANG XUE (薛会芳) ^{1,2,3} AND JIA-SHU NIU (牛家树) ^{4,5,6}

¹*Department of Physics, Taiyuan Normal University, Jinzhong 030619, China*

²*Institute of Computational and Applied Physics, Taiyuan Normal University, Jinzhong 030619, China*

³*Shanxi Key Laboratory for Intelligent Optimization Computing and Blockchain Technology, Jinzhong 030619, China*

⁴*Institute of Theoretical Physics, Shanxi University, Taiyuan 030006, China*

⁵*State Key Laboratory of Quantum Optics and Quantum Optics Devices, Shanxi University, Taiyuan 030006, China*

⁶*Collaborative Innovation Center of Extreme Optics, Shanxi University, Taiyuan, Shanxi 030006, China*

ABSTRACT

Harmonics are a ubiquitous feature across various pulsating stars, traditionally viewed as mere replicas of the independent primary pulsation modes, and have thus been excluded from asteroseismological models. Recent research, however, has uncovered a significant discrepancy: in high-amplitude δ Scuti stars (HADS), harmonics exhibit uncorrelated variations in amplitude and frequency relative to their parent modes. The serendipitous nature of these disharmonized harmonics is a question of critical importance. In our study, we analyzed five triple-mode HADS stars observed by the Transiting Exoplanet Survey Satellite (TESS) and discovered some pervasive patterns of disharmonized harmonics in both the fundamental (f_0) and first overtone (f_1) pulsation modes. Intriguingly, through an in-depth frequency interaction analysis of V1393 Cen, we identified $2f_1$ as an independent pulsation mode, distinct from f_1 , and pinpointed it as the progenitor of the frequency variations observed in $3f_1$, $4f_1$, $5f_1$, and $6f_1$. Notably, we found an interesting pattern in decomposing of the harmonics, which uncovers the generation process of harmonics for the first time. These findings serve as a new window on the research of harmonics, which remains a hidden corner of contemporary asteroseismology.

1. INTRODUCTION

Harmonics, associated with independent pulsation modes, are a prevalent phenomenon in the constellation of pulsating stars, encompassing a diverse array that includes Cepheids (Rathour et al. 2021), RR Lyrae stars (Kurtz et al. 2016), δ Scuti stars (Breger & Montgomery 2014), γ Dor stars (Kurtz et al. 2015), pulsating white dwarfs (Wu 2001), β Cep stars (Degroote et al. 2009), and slowly pulsating B stars (Pápics et al. 2017). Traditionally, these harmonics have been ascribed to the light curves' nonsinusoidal patterns, a manifestation of the stellar medium's nonlinear response to the propagation of pulsation waves. Consequently, they are not classified as intrinsic stellar pulsation modes (Brickhill 1992; Wu 2001) and are presumed to faithfully replicate the characteristics of their independent parent modes.

δ Scuti stars, known for their short-period pulsations, span periods from 15 minutes to 8 hours and are classi-

fied within spectral types A through F. They are located at the confluence of the main sequence (MS) and the lower boundary of the classical Cepheid instability strip on the Hertzsprung-Russell diagram. The pulsations in these stars are self-excited through the κ mechanism, stemming from the partial ionization of helium in the outer layers (Kallinger et al. 2008; Handler 2009; Guenther et al. 2009; Uytterhoeven et al. 2011; Holdsworth et al. 2014; Steindl et al. 2022).

The high-amplitude δ Scuti stars (HADS) represent a distinct subclass within the δ Scuti stars, characterized by more pronounced amplitudes ($\Delta V \geq 0^m 1$) and slower rotation speeds ($v \sin i \leq 30$ km/s), although the accumulation of more HADS samples has blurred these traditional distinctions (Balona et al. 2012). The majority of HADS oscillate with one or two radial pulsation modes (Niu et al. 2013, 2017; Xue et al. 2018; Bowman et al. 2021; Daszyńska-Daszkiewicz et al. 2022; Xue et al. 2022), yet a subset exhibits more complex pulsation patterns, including three radial modes (Wils et al. 2008; Niu & Xue 2022; Xue et al. 2023), four radial modes (Pietrukowicz et al. 2013; Netzel et al. 2022; Netzel &

Smolec 2022), and even non-radial modes (Poretti et al. 2011; Xue & Niu 2020).

In the case of the SX Phe star (a Population II subclass of HADS), XX Cyg, which features a periodogram dominated by the fundamental pulsation mode (f_0) and its 19 harmonics, Niu et al. (2023) discovered that the harmonics exhibit significant and uncorrelated amplitude and frequency variations over time, with these variations becoming more pronounced with increasing harmonic order. Furthermore, for the radial triple-mode HADS KIC 6382916, the harmonics of the fundamental and first overtone pulsation modes (f_0 and f_1) display uncorrelated amplitude and frequency variations relative to their parent modes, even for the first and second harmonics ($2f_0$, $3f_0$, $2f_1$ and $3f_1$) (Niu & Xue 2024). We refer to these as disharmonized harmonic pulsation modes, or simply, disharmonized harmonics.

These disharmonized harmonics challenge the conventional wisdom regarding the behavior of harmonics and expose an unexplored aspect of asteroseismology. The question of whether these disharmonized harmonics are a specific feature of certain pulsating stars or represent a widespread phenomenon across certain types of pulsating stars is a critical inquiry in contemporary research.

In this study, we scrutinize the amplitude and frequency variations of the harmonics in five HADS stars: DO CMi, GSC 06047-00749 (ASAS J094303-1707.3), V0803 Aur, V1384 Tau, and V1393 Cen. These stars have been identified as radial triple-mode HADS based on continuous time-series photometric data from the TESS space telescope (Xue et al. 2023).

2. METHODS

All the five HADS under investigation were observed by TESS, with their flux measurements obtained from the MAST Portal¹ and processed by the TESS Science Processing Operations Center (SPOC; Jenkins et al. (2016)). We converted the normalized fluxes to magnitudes using the TESS magnitude system and eliminated long-term trends for each sector. Subsequently, we selected the light curves with the most data points in a single sector for each star, as detailed in Table 1. Fourier analysis was applied to these light curves, and the resulting amplitudes and frequencies for the fundamental, first overtone, and second overtone pulsation modes (A_0 , A_1 , A_2 and f_0 , f_1 , f_2) are presented in the same table.

¹ <https://mast.stsci.edu/portal/Mashup/Clients/Mast/Portal.html>

To elucidate the temporal variations in the amplitudes and frequencies of the harmonics, we employed the short-time Fourier transform, as described in detail by Niu & Xue (2022); Niu et al. (2023); Niu & Xue (2024). A pre-whitening process was executed within an 8-day time window, which was advanced in increments of 0.2 days across the entire dataset. At each step, the pre-whitening process was utilized to obtain the amplitudes and frequencies of the independent pulsation modes and their harmonics, with the phase considered as a free parameter, not the primary focus of this study.

The pre-whitening process was performed through Fourier decomposition, as represented by the following equation:

$$m = m_0 + \sum A_i \sin [2\pi(f_i t + \phi_i)], \quad (1)$$

where m_0 denotes the shifted value, A_i represents the amplitude, f_i is the frequency, and ϕ_i corresponds to the phase. The amplitude uncertainties (σ_a) were determined as the median amplitude value within a spectral window of 4 c/d, divided equally by the frequency peak, in line with methods described by Niu et al. (2023); Niu & Xue (2024). Frequency uncertainties (σ_f) were estimated based on the relationship between amplitude and frequency as proposed by Montgomery & O'Donoghue (1999) and Aerts (2021), as shown in the equation below:

$$\sigma_f = \sigma_a \cdot \frac{\sqrt{3}}{\pi \cdot A \cdot T}, \quad (2)$$

where A is the amplitude and T represents the total time baseline used in the pre-whitening process.

Ultimately, we extracted the variation data (amplitudes and frequencies) for the fundamental and first overtone pulsation modes and their harmonics (denoted as $m f_0$ and $n f_1$, where $m, n \in \mathbb{N}$ and $m, n > 1$) for the five HADS. The precise number of harmonics was contingent upon the signal-to-noise ratio within the moving time windows, with no significant signals detected for the harmonics of the second overtone pulsation mode.

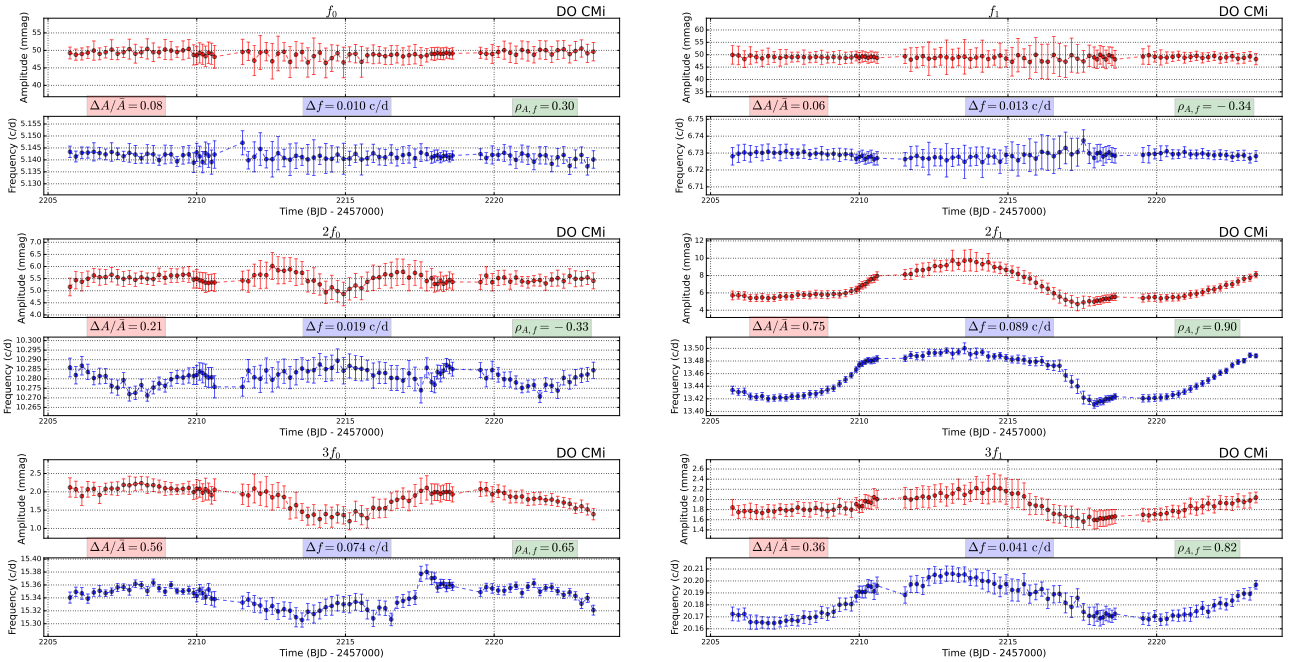
3. RESULTS

The variations in amplitude and frequency for the fundamental, first overtone, and their associated harmonic pulsation modes in DO CMi and V1393 Cen are depicted in Figures 1 (DO CMi: $f_0 - 3f_0$ and $f_1 - 3f_1$) and 2 (V1393 Cen: $f_0 - 3f_0$ and $f_1 - 6f_1$), respectively. The corresponding data for the remaining three HADS stars are presented in the Appendix, specifically in Figures A1 (GSC 06047-00749: $f_0 - 3f_0$ and $f_1 - 4f_1$), A2 (V0803 Aur: $f_0 - 4f_0$ and $f_1 - 2f_1$), and A3 (V1384 Tau: $f_0 - 3f_0$ and $f_1 - 3f_1$).

To quantitatively illustrate the variations in amplitude and frequency, as well as their interrelations, we have

Table 1. Amplitudes and frequencies of the fundamental, first overtone, and second overtone pulsation modes of the five triple-mode HADS.

| ID | DO CMi | GSC 06047-00749 | V0803 Aur | V1384 Tau | V1393 Cen |
|--------------|---------------------|----------------------|----------------------|----------------------|----------------------|
| A_0 (mmag) | 49 ± 1 | 53 ± 1 | 49.5 ± 0.6 | 52.8 ± 0.8 | 41.3 ± 0.5 |
| f_0 (c/d) | 5.1416 ± 0.0005 | 10.0829 ± 0.0004 | 14.0735 ± 0.0003 | 7.1534 ± 0.0003 | 8.4902 ± 0.0003 |
| A_1 (mmag) | 49.0 ± 0.7 | 61 ± 1 | 20.8 ± 0.2 | 49.9 ± 0.5 | 71 ± 1 |
| f_1 (c/d) | 6.7284 ± 0.0003 | 13.0690 ± 0.0005 | 18.1716 ± 0.0003 | 9.3117 ± 0.0002 | 11.0093 ± 0.0003 |
| A_2 (mmag) | 11.6 ± 0.2 | 1.42 ± 0.07 | 4.5 ± 0.1 | 4.41 ± 0.07 | 5.65 ± 0.09 |
| f_2 (c/d) | 8.6078 ± 0.0004 | 16.303 ± 0.001 | 22.5272 ± 0.0005 | 11.6430 ± 0.0003 | 13.7271 ± 0.0003 |
| TESS Sector | 33 (600 s) | 62 (200 s) | 43 (120 s) | 05 (120 s) | 11 (120 s) |


Figure 1. Amplitude and frequency variations of the fundamental, first overtone, and their harmonic pulsation modes ($f_0 - 3f_0$ and $f_1 - 3f_1$) in DO CMi.

calculated the relative amplitude variations ($\Delta A/\bar{A} \equiv (A_{\max} - A_{\min})/\bar{A}$)², the absolute frequency variations ($\Delta f \equiv f_{\max} - f_{\min}$)³, and the Pearson correlation coefficient ($\rho_{A,f}$) between amplitude and frequency. These quantitative metrics are displayed in Figures 1, 2, A1, A2, and A3, providing a detailed account of the observed phenomena.

4. DISCUSSIONS

² Here, A_{\max} and A_{\min} represent the maximum and minimum amplitude values within the moving windows, while \bar{A} denotes the mean amplitude across these windows.

³ f_{\max} and f_{\min} correspond to the maximum and minimum frequency values observed within the moving windows.

Typically, the amplitudes and frequencies of the fundamental (f_0) and first overtone (f_1) pulsation modes exhibit a high degree of stability over a timescale of more than ten days. However, a marked deviation from this stability is observed as the order of the harmonics increases, suggesting the presence of yet unidentified mechanisms. This phenomenon is particularly prevalent among triple-mode HADS, where disharmonized harmonics are commonly encountered.

On a finer timescale of approximately 0.2 to 1.0 days, minor frequency modulations become apparent, affecting certain pulsation modes. This effect is notably evident in DO CMi (f_0 and f_1), V1393 Cen (f_1 and $3f_1$), GSC 06047-00749 (f_1), and V1384 Tau (f_0). The observation of a similar 0.6570-day modulation in the time-

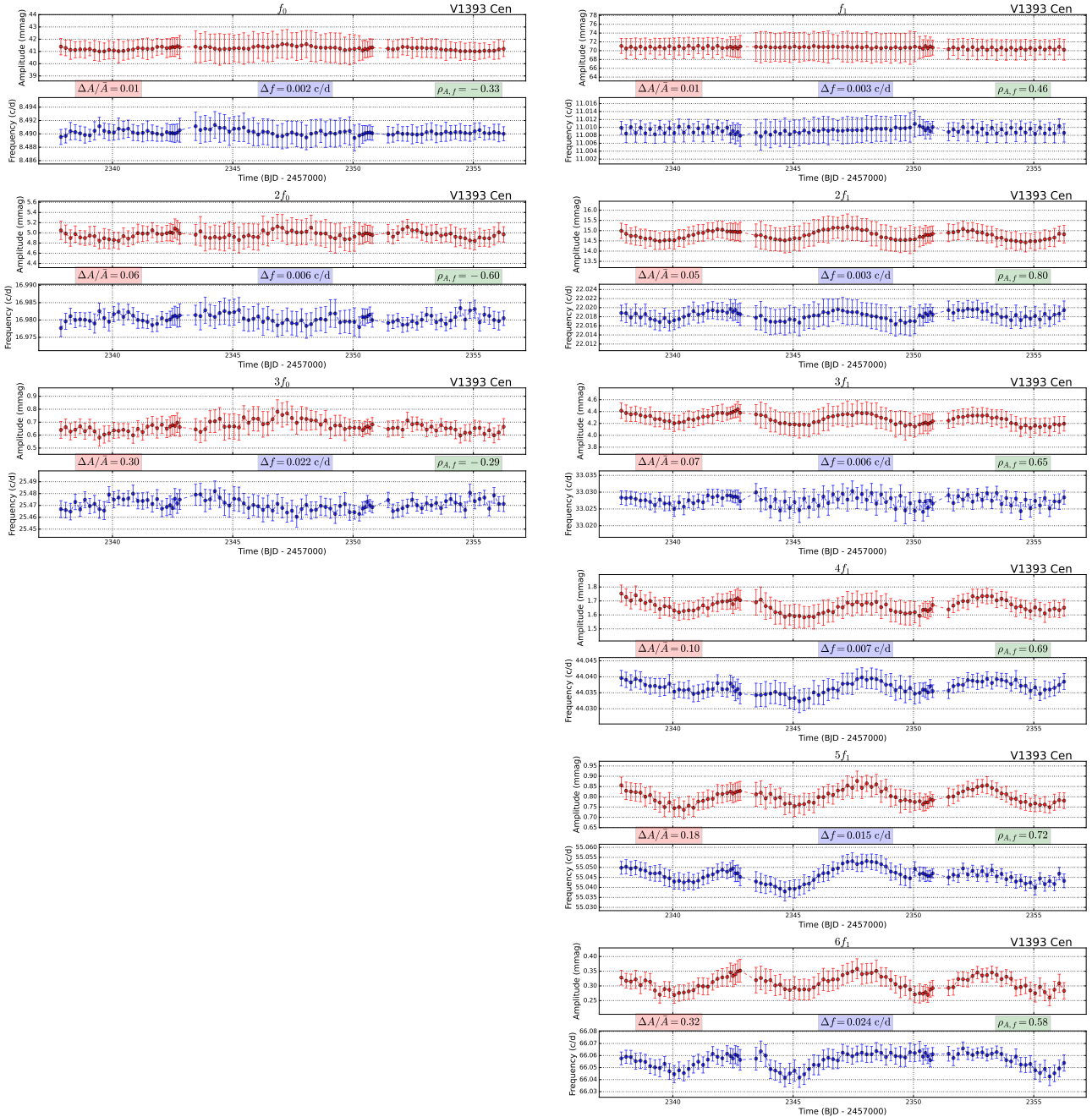


Figure 2. Amplitude and frequency variations of the fundamental, first overtone, and their harmonic pulsation modes ($f_0 - 3f_0$ and $f_1 - 6f_1$) in V1393 Cen.

frequency diagram of KIC 6382916 (Niu & Xue 2024) indicates that such modulations may be a common characteristic of triple-mode HADS, although the underlying physical processes remain elusive.

The disharmonized harmonics exhibit distinct behaviors for f_0 and f_1 . For f_0 , the amplitude and frequency variations of its harmonics do not exhibit a strong correlation, as seen with $2f_0$ and $3f_0$ in DO CMi. In contrast, for f_1 , there is a significant correlation in the amplitude and frequency variations, particularly evident in

DO CMi ($2f_1$ and $3f_1$) and V1393 Cen ($2f_1$, $3f_1$, $4f_1$, $5f_1$, and $6f_1$).

An intriguing observation is the significant (anti)correlated relationships in the variations of amplitude and frequency for certain pulsation modes, as precisely quantified by the Pearson correlation coefficient ($\rho_{A,f}$) presented in the figures. This is notably observed in DO CMi ($3f_0$, $2f_1$, and $3f_1$), V1393 Cen ($2f_0$, $2f_1$, $3f_1$, $4f_1$, $5f_1$, $6f_1$), and GSC 06047-00749 ($3f_1$ and $4f_1$). These (anti)correlations are significant

as they suggest that the observed amplitude and frequency variations may be attributed to modulations resulting from interactions among pulsation modes (Niu & Xue 2024).

The harmonics of f_1 in V1393 Cen, which display a high degree of correlation, provide a valuable context for exploring the detailed relationships among all f_0 and f_1 harmonics. This is achieved through the interaction diagram of frequencies (Figure 3)⁴. The frequency variations of the pulsation modes are grouped into two distinct categories: those related to f_0 and those related to f_1 . As depicted in Figure 3, all f_1 -related harmonics, with the exception of f_1 itself, exhibit significant correlations. This is analogous to the findings for KIC 6382916 (Niu & Xue 2024), where $2f_1$ is considered an independent parent mode for $3f_1$ due to their significant correlation. The correct representation of $3f_1$ should thus be $(2f_1) + (f_1)$ rather than $3 \cdot (f_1)$.⁵

Applying the principle that a harmonic's parent mode should exhibit the highest correlation in frequency variations, we can deduce the correct representation of all harmonics as follows:

$$\begin{aligned} (6f_1) &= (5f_1) + (f_1); \\ (5f_1) &= (4f_1) + (f_1); \\ (4f_1) &= (3f_1) + (f_1); \\ (3f_1) &= (2f_1) + (f_1). \end{aligned} \quad (3)$$

Each of these high-order harmonics (nf_1 , $n \geq 3$) have two parent modes, one is f_1 , the other is $(n-1)f_1$ (which passes on its patterns of variation to nf_1). What's even more interesting from a global perspective is that these higher-order harmonics seem to be generated step by step, i.e. nf_1 is directly generated by $(n-1)f_1$ rather than the lower order harmonics. This interesting generation mechanism of harmonics interprets the ubiquitous phenomenon in the spectrogram of many pulsating stars: harmonics appear one by one in order, whose amplitude decrease as the order increase.

However, the relationship

$$(2f_1) \neq (f_1) + (f_1), \quad (4)$$

holds true due to the negative correlation coefficient (-0.16) between f_1 and $2f_1$. Consequently, considering the frequency variations, $2f_1$ emerges as an independent pulsation mode, the progenitor of the significant

frequency variations observed in higher-order harmonics. This pattern is also evident in KIC 6382916 (Niu & Xue 2024) and DO CMi (as shown in Figure 1).

The origin of the frequency variations of $2f_1$ needs further investigation and may be linked to the nature of f_2 as a resonating integration mode, as well as the resonance relationship among f_0 , f_1 , and f_2 , as expressed by the equation:

$$2f_1 - f_0 = f_2 - \Delta\omega, \quad (5)$$

where $\Delta\omega$ represents the star's rotational frequency. Elucidating the details of this relationship is an area earmarked for future research.

In summary, the present study has provided compelling evidence for the prevalence of disharmonized harmonics in HADS, challenging the traditional paradigm of harmonic behavior in pulsating stars. The detailed analysis of five triple-mode HADS stars, has unveiled a complex pattern of amplitude and frequency variations that cannot be solely attributed to the independent parent pulsation modes. The discovery of $2f_1$ as an independent pulsation mode, with its own intrinsic frequency variations, suggests the existence of a multifaceted mechanism governing the pulsations. An intuitive but non-trivial discovery uncovers the generation process of the harmonics. These findings call for a reassessment of the current models and invite further investigation into the underlying physics, potentially leading to a more comprehensive understanding of the pulsation phenomena in δ Scuti stars and other variable stars.

ACKNOWLEDGMENTS

H.F.X. acknowledges support from the National Natural Science Foundation of China (NSFC) (No. 12303036) and the Applied Basic Research Programs of Natural Science Foundation of Shanxi Province (No. 202103021223320). J.S.N. acknowledges support from the National Natural Science Foundation of China (NSFC) (No. 12005124). The authors acknowledge the TESS Science team and everyone who has contributed to making the TESS mission possible.

Software: `astropy` (Astropy Collaboration et al. 2022), `Lightkurve` (Lightkurve Collaboration et al. 2018), `NumPy` (Harris et al. 2020), `SciPy` (Virtanen et al. 2020), `matplotlib` (Hunter 2007)

⁴ For subsequent quantitative analysis, the correlation coefficients between frequency variations are filled in the colored squares for reference.

⁵ The parentheses here indicate that the enclosed pulsation modes should be regarded as a collective entity rather than mere multiples of f_1 .

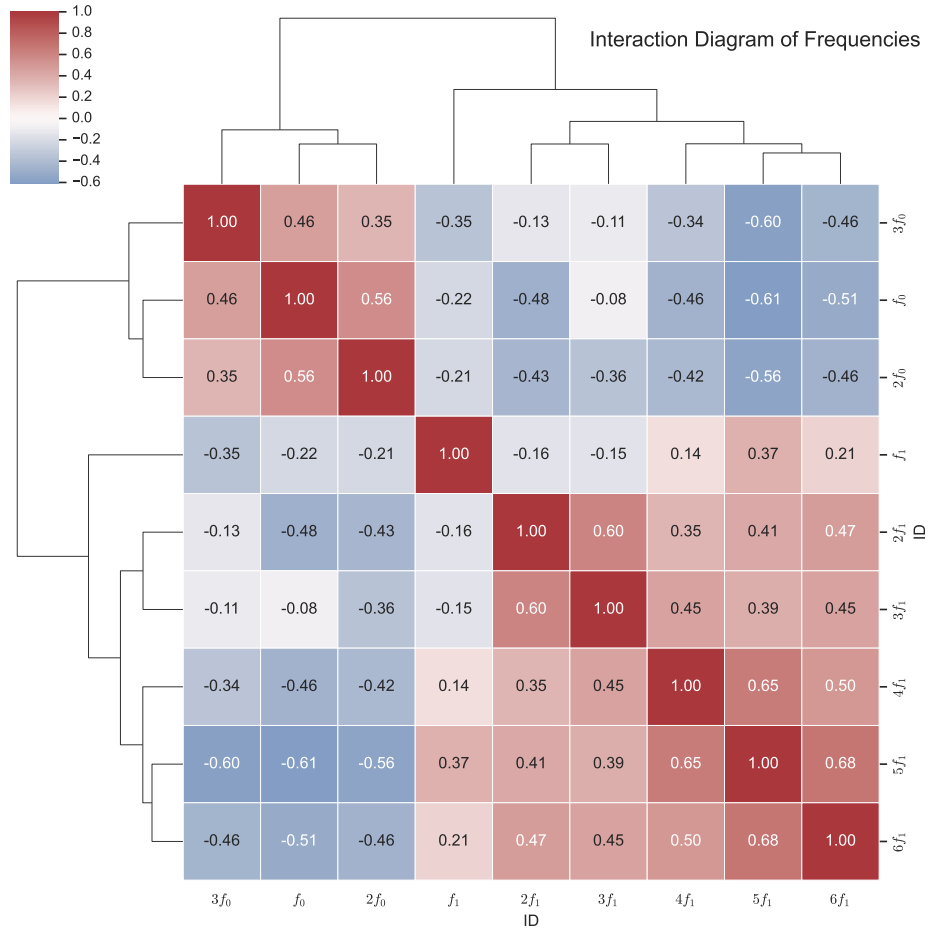


Figure 3. Interaction diagram of frequencies of the f_0 , f_1 , and their harmonic pulsation modes in V1393 Cen.

REFERENCES

- Aerts, C. 2021, *Rev. Mod. Phys.*, 93, 015001, doi: [10.1103/RevModPhys.93.015001](https://doi.org/10.1103/RevModPhys.93.015001)
- Astropy Collaboration, Price-Whelan, A. M., Lim, P. L., et al. 2022, *ApJ*, 935, 167, doi: [10.3847/1538-4357/ac7c74](https://doi.org/10.3847/1538-4357/ac7c74)
- Balona, L. A., Lenz, P., Antoci, V., et al. 2012, *MNRAS*, 419, 3028, doi: [10.1111/j.1365-2966.2011.19939.x](https://doi.org/10.1111/j.1365-2966.2011.19939.x)
- Bowman, D. M., Hermans, J., Daszyńska-Daszkiewicz, J., et al. 2021, *MNRAS*, 504, 4039, doi: [10.1093/mnras/stab1124](https://doi.org/10.1093/mnras/stab1124)
- Breger, M., & Montgomery, M. H. 2014, *ApJ*, 783, 89, doi: [10.1088/0004-637X/783/2/89](https://doi.org/10.1088/0004-637X/783/2/89)
- Brickhill, A. J. 1992, *MNRAS*, 259, 519, doi: [10.1093/mnras/259.3.519](https://doi.org/10.1093/mnras/259.3.519)
- Daszyńska-Daszkiewicz, J., Walczak, P., Pamyatnykh, A. A., & Szewczuk, W. 2022, *MNRAS*, 512, 3551, doi: [10.1093/mnras/stac646](https://doi.org/10.1093/mnras/stac646)
- Degroote, P., Briquet, M., Catala, C., et al. 2009, *A&A*, 506, 111, doi: [10.1051/0004-6361/200911782](https://doi.org/10.1051/0004-6361/200911782)
- Guenther, D. B., Kallinger, T., Zwintz, K., et al. 2009, *ApJ*, 704, 1710, doi: [10.1088/0004-637X/704/2/1710](https://doi.org/10.1088/0004-637X/704/2/1710)
- Handler, G. 2009, in *American Institute of Physics Conference Series*, Vol. 1170, *Stellar Pulsation: Challenges for Theory and Observation*, ed. J. A. Guzik & P. A. Bradley, 403–409, doi: [10.1063/1.3246528](https://doi.org/10.1063/1.3246528)
- Harris, C. R., Millman, K. J., van der Walt, S. J., et al. 2020, *Nature*, 585, 357, doi: [10.1038/s41586-020-2649-2](https://doi.org/10.1038/s41586-020-2649-2)
- Holdsworth, D. L., Smalley, B., Gillon, M., et al. 2014, *MNRAS*, 439, 2078, doi: [10.1093/mnras/stu094](https://doi.org/10.1093/mnras/stu094)
- Hunter, J. D. 2007, *Computing in Science and Engineering*, 9, 90, doi: [10.1109/MCSE.2007.55](https://doi.org/10.1109/MCSE.2007.55)
- Jenkins, J. M., Twicken, J. D., McCauliff, S., et al. 2016, in *Society of Photo-Optical Instrumentation Engineers (SPIE) Conference Series*, Vol. 9913, *Software and Cyberinfrastructure for Astronomy IV*, ed. G. Chiozzi & J. C. Guzman, 99133E, doi: [10.1117/12.2233418](https://doi.org/10.1117/12.2233418)
- Kallinger, T., Zwintz, K., & Weiss, W. 2008, *A&A*, 488, 279, doi: [10.1051/0004-6361/20079207](https://doi.org/10.1051/0004-6361/20079207)
- Kurtz, D. W., Bowman, D. M., Ebo, S. J., et al. 2016, *MNRAS*, 455, 1237, doi: [10.1093/mnras/stv2377](https://doi.org/10.1093/mnras/stv2377)
- Kurtz, D. W., Shibahashi, H., Murphy, S. J., Bedding, T. R., & Bowman, D. M. 2015, *MNRAS*, 450, 3015, doi: [10.1093/mnras/stv868](https://doi.org/10.1093/mnras/stv868)
- Lightkurve Collaboration, Cardoso, J. V. d. M., Hedges, C., et al. 2018, *Lightkurve: Kepler and TESS time series analysis in Python*, *Astrophysics Source Code Library*, record ascl:1812.013. <http://ascl.net/1812.013>
- Montgomery, M. H., & O’Donoghue, D. 1999, *Delta Scuti Star Newsletter*, 13, 28
- Netzel, H., Pietrukowicz, P., Soszyński, I., & Wrona, M. 2022, *MNRAS*, 510, 1748, doi: [10.1093/mnras/stab3555](https://doi.org/10.1093/mnras/stab3555)
- Netzel, H., & Smolec, R. 2022, *MNRAS*, 515, 4574, doi: [10.1093/mnras/stac1938](https://doi.org/10.1093/mnras/stac1938)
- Niu, J.-S., Fu, J.-N., & Zong, W.-K. 2013, *Res. Astron. Astrophys.*, 13, 1181, doi: [10.1088/1674-4527/13/10/004](https://doi.org/10.1088/1674-4527/13/10/004)
- Niu, J.-S., Liu, Y., & Xue, H.-F. 2023, *AJ*, 166, 43, doi: [10.3847/1538-3881/acda2b](https://doi.org/10.3847/1538-3881/acda2b)
- Niu, J.-S., & Xue, H.-F. 2022, *ApJL*, 938, L20, doi: [10.3847/2041-8213/ac9407](https://doi.org/10.3847/2041-8213/ac9407)
- . 2024, *A&A*, 628, L8, doi: [10.1051/0004-6361/202348757](https://doi.org/10.1051/0004-6361/202348757)
- Niu, J.-S., Fu, J.-N., Li, Y., et al. 2017, *MNRAS*, 467, 3122, doi: [10.1093/mnras/stx125](https://doi.org/10.1093/mnras/stx125)
- Pápics, P. I., Tkachenko, A., Van Reeth, T., et al. 2017, *A&A*, 598, A74, doi: [10.1051/0004-6361/201629814](https://doi.org/10.1051/0004-6361/201629814)
- Pietrukowicz, P., Dziembowski, W. A., Mróz, P., et al. 2013, *AcA*, 63, 379, doi: [10.48550/arXiv.1311.5894](https://doi.org/10.48550/arXiv.1311.5894)
- Poretti, E., Rainer, M., Weiss, W. W., et al. 2011, *A&A*, 528, A147, doi: [10.1051/0004-6361/201016045](https://doi.org/10.1051/0004-6361/201016045)
- Rathour, R. S., Smolec, R., & Netzel, H. 2021, *MNRAS*, 505, 5412, doi: [10.1093/mnras/stab1603](https://doi.org/10.1093/mnras/stab1603)
- Steindl, T., Zwintz, K., & Vorobyov, E. 2022, *Nature Communications*, 13, 5355, doi: [10.1038/s41467-022-32882-0](https://doi.org/10.1038/s41467-022-32882-0)
- Uytterhoeven, K., Moya, A., Grigahcène, A., et al. 2011, *A&A*, 534, A125, doi: [10.1051/0004-6361/201117368](https://doi.org/10.1051/0004-6361/201117368)
- Virtanen, P., Gommers, R., Oliphant, T. E., et al. 2020, *Nature Methods*, 17, 261, doi: [10.1038/s41592-019-0686-2](https://doi.org/10.1038/s41592-019-0686-2)
- Wils, P., Rozakis, I., Kleidis, S., Hamsch, F. J., & Bernhard, K. 2008, *A&A*, 478, 865, doi: [10.1051/0004-6361:20078992](https://doi.org/10.1051/0004-6361:20078992)
- Wu, Y. 2001, *MNRAS*, 323, 248, doi: [10.1046/j.1365-8711.2001.04224.x](https://doi.org/10.1046/j.1365-8711.2001.04224.x)
- Xue, H.-F., & Niu, J.-S. 2020, *ApJ*, 904, 5, doi: [10.3847/1538-4357/abbc12](https://doi.org/10.3847/1538-4357/abbc12)
- Xue, H.-F., Niu, J.-S., & Fu, J.-N. 2022, *Res. Astron. Astrophys.*, 22, 105006, doi: [10.1088/1674-4527/ac8b5e](https://doi.org/10.1088/1674-4527/ac8b5e)
- Xue, H.-F., Fu, J.-N., Fox-Machado, L., et al. 2018, *ApJ*, 861, 96, doi: [10.3847/1538-4357/aac9c5](https://doi.org/10.3847/1538-4357/aac9c5)
- Xue, W., Niu, J.-S., Xue, H.-F., & Yin, S. 2023, *Res. Astron. Astrophys.*, 23, 075002, doi: [10.1088/1674-4527/accdbc](https://doi.org/10.1088/1674-4527/accdbc)

APPENDIX

A. ADDITIONAL FIGURES

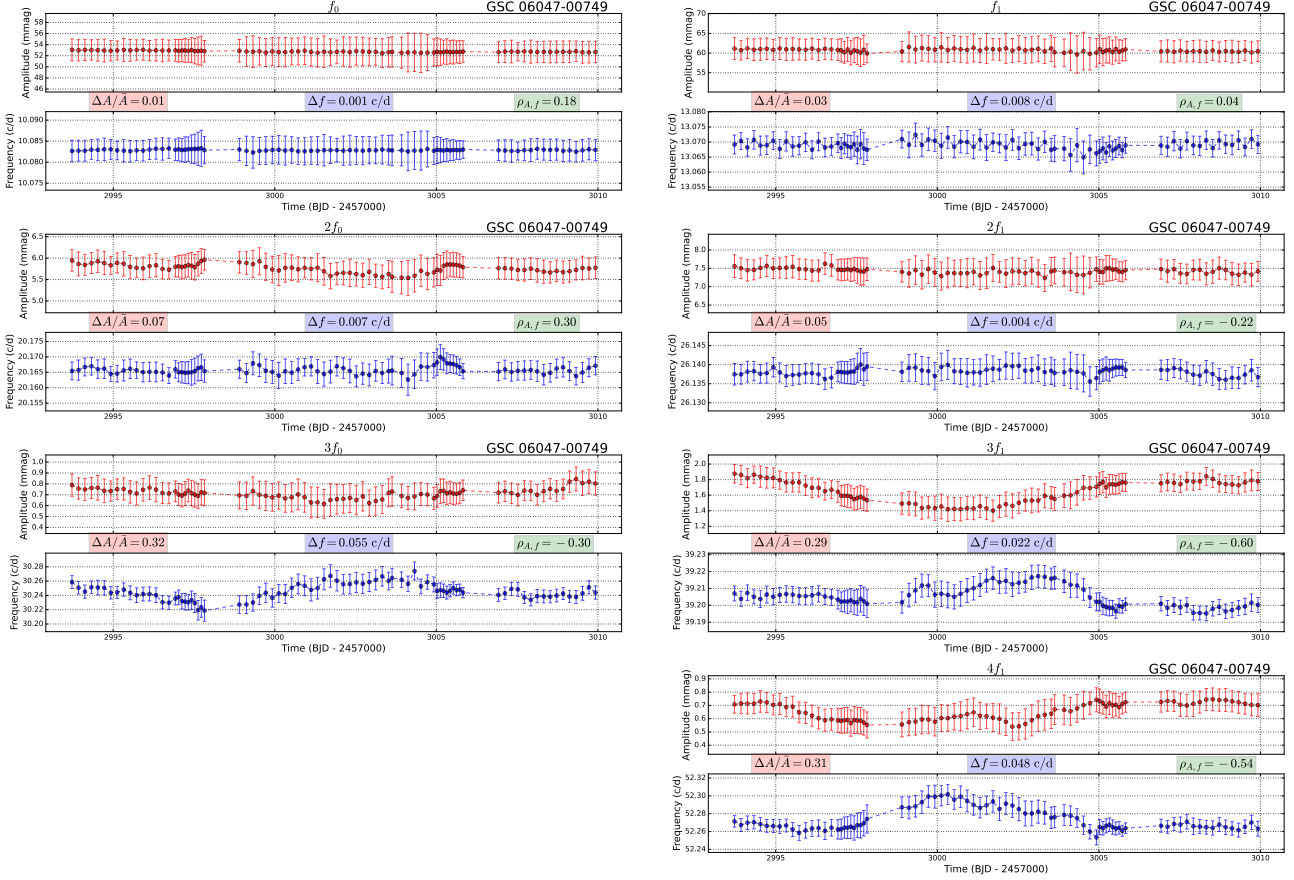


Figure A1. Amplitude and frequency variations of the fundamental, first overtone, and their harmonic pulsation modes ($f_0 - 3f_0$ and $f_1 - 4f_1$) in GSC 06047-00749.

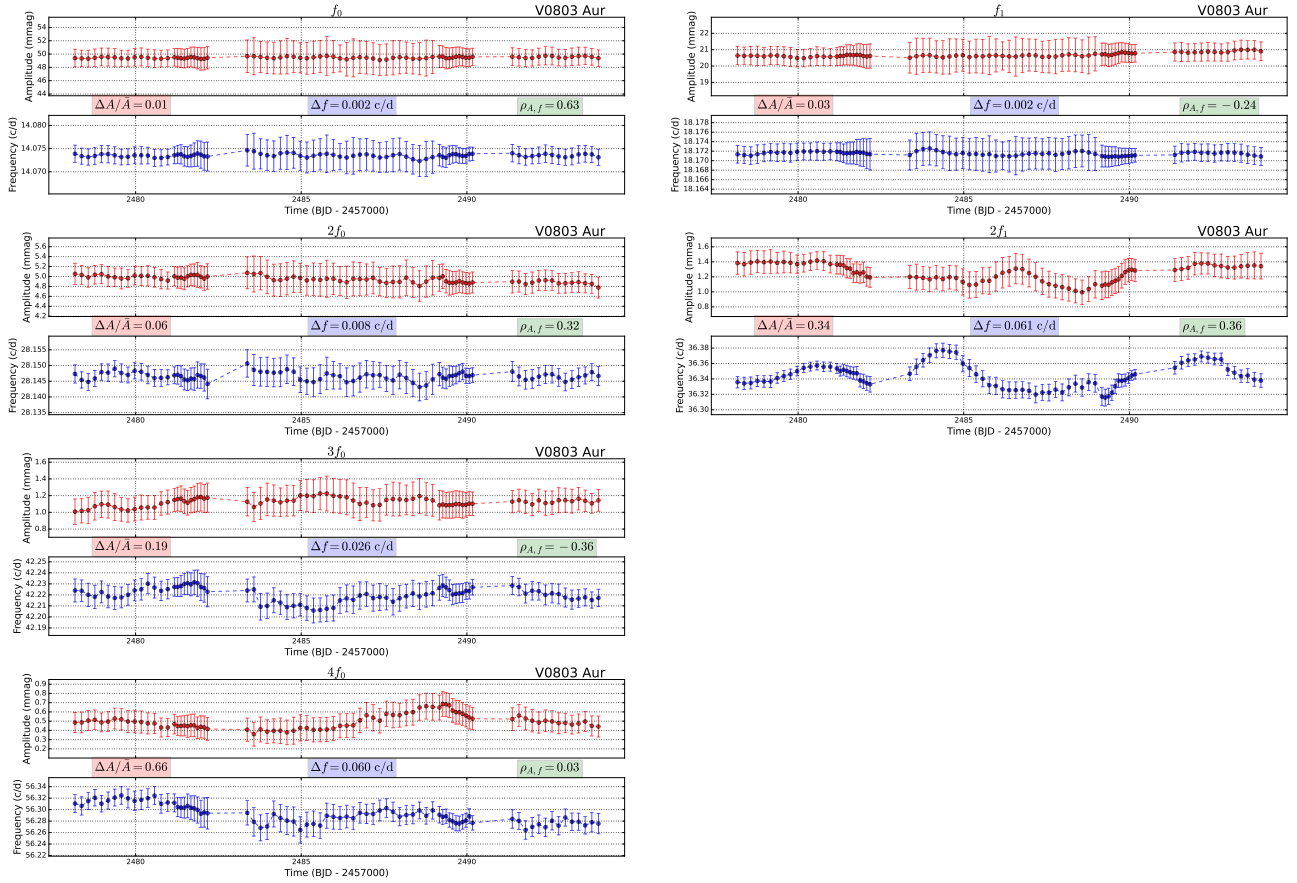


Figure A2. Amplitude and frequency variations of the fundamental, first overtone, and their harmonic pulsation modes ($f_0 - 4f_0$ and $f_1 - 2f_1$) in V0803 Aur.

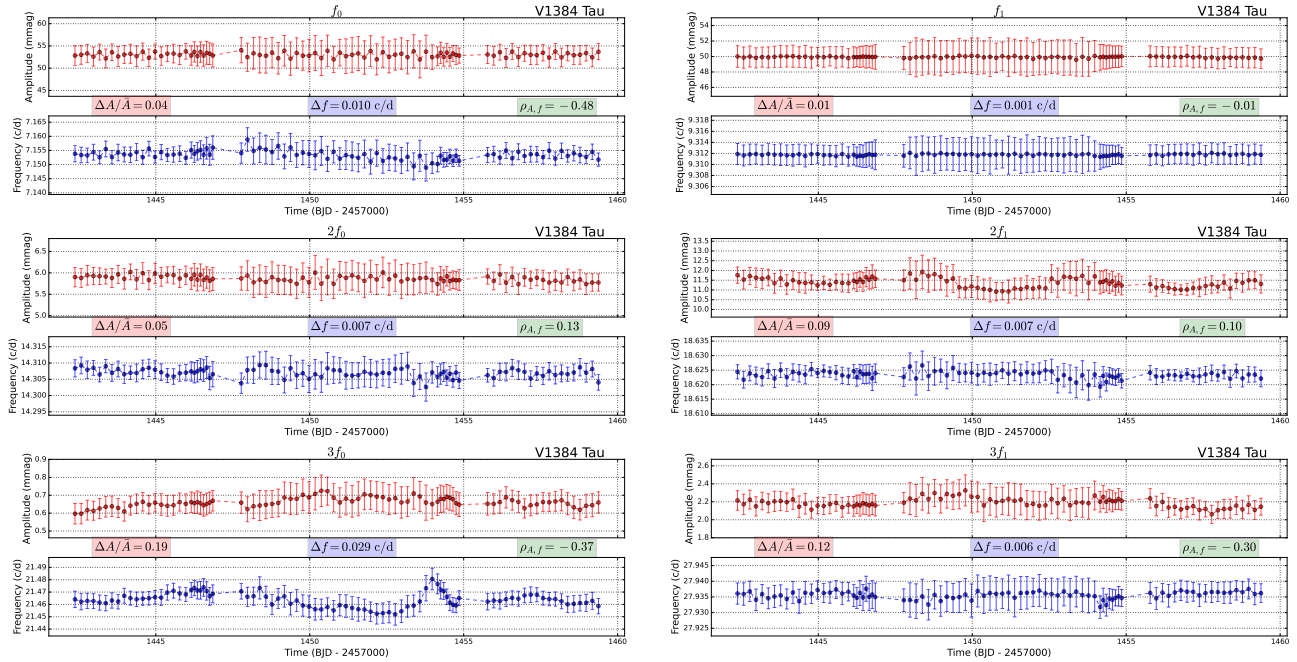


Figure A3. Amplitude and frequency variations of the fundamental, first overtone, and their harmonic pulsation modes ($f_0 - 3f_0$ and $f_1 - 3f_1$) in V1384 Tau.